

ORIGINAL ARTICLE

Open Access



Effect of thermal oxidation on the dry sliding friction and wear behaviour of CP-Ti on CP-Ti tribopairs

Yong Sun^{1*} , Richard Bailey¹, Jin Zhang², Yong Lian² and Xiulin Ji³

Abstract

Thermal oxidation (TO) has proven to be a cost-effective and efficient technique to engineer the surfaces of titanium and its alloys to achieve enhanced surface properties. The benefits of TO treatment in enhancing the tribological properties of titanium have been demonstrated by many investigators. However, most of the reported tribological studies have been based on the contact between a TO treated titanium specimen and a counter-body made of other materials, mainly ceramics, steels and polymers. Very few studies have been reported on the friction and wear behaviour of TO treated titanium sliding against TO treated titanium. In this work, the effect of thermal oxidation on the dry sliding friction and wear behaviour of commercially pure Ti (CP-Ti) on CP-Ti tribopairs was investigated under loading conditions ranging from elastic contact to plastic contact. Comparisons were made among three contact pairs: (1) untreated Ti on untreated Ti (Ti-Ti), (2) untreated Ti on TO treated Ti (Ti-TO) and (3) TO treated Ti on TO treated Ti (TO-TO). The results show that the TO-TO contact pair presents an ideal material combination to achieve the best tribological performance in terms of low friction and superior wear resistance. On the other hand, the Ti-Ti pair presents the worst combination in terms of tribological performance. While the Ti-TO pair performs better than the Ti-Ti pair tribologically, it is not as good as the TO-TO pair. It is essential to thermally oxidize both specimens in order to achieve optimal tribological performance. It is the oxide layer-on-oxide layer contact that imparts the excellent tribological performance. Failure of the oxide layer in one of the contact bodies can lead to high and unstable friction and increased wear from both contacting bodies. The tribological performance of the three contact pairs and the failure mechanism of the oxide layer are discussed in the paper. The results of this work suggest that the TO treated Ti on TO treated Ti contact pair would have potential tribological applications in engineering.

Keywords Titanium, Thermal oxidation, Self-mating, Friction, Wear, Dry sliding

1 Introduction

Titanium is a desirable engineering material because of its light weight, high strength, excellent corrosion resistance and biocompatibility. Due to the high strength-to-density ratio, the use of titanium and its alloys in the transportation and aerospace sectors can result in considerable weight-saving and thus energy-saving. However, titanium is notorious for its poor tribological properties [1–3]. When in sliding contact with itself and other materials, titanium tends to gall severely, resulting in high and unstable friction, large amounts of wear and the possibility of seizure. Thus, the uses of titanium

*Correspondence:

Yong Sun

ysun01@dmu.ac.uk

¹ School of Engineering and Sustainable Development, Faculty of Computing, Engineering and Media, De Montfort University, Leicester LE1 9BH, UK

² Institute of Advanced Materials Technology, University of Science and Technology Beijing, Beijing 100083, China

³ Department of Mechatronics Engineering, Shantou University, Shantou 525063, China



© The Author(s) 2023. **Open Access** This article is licensed under a Creative Commons Attribution 4.0 International License, which permits use, sharing, adaptation, distribution and reproduction in any medium or format, as long as you give appropriate credit to the original author(s) and the source, provide a link to the Creative Commons licence, and indicate if changes were made. The images or other third party material in this article are included in the article's Creative Commons licence, unless indicated otherwise in a credit line to the material. If material is not included in the article's Creative Commons licence and your intended use is not permitted by statutory regulation or exceeds the permitted use, you will need to obtain permission directly from the copyright holder. To view a copy of this licence, visit <http://creativecommons.org/licenses/by/4.0/>.

have been restricted to mostly non-tribological applications. It is still difficult to make power transmission components, such as gears and bearings from titanium and its alloys. Such a poor tribological behaviour of titanium has long been the subject of investigations with many factors being identified as contributing towards its high and unstable friction and severe adhesive wear. It has been suggested that a combined effect of electron configuration, high chemical reactivity, crystal structure, poor thermal conductivity, lubrication ineffectiveness results in a high level of adhesive wear associated with a large amount of material transfer when subjected to tribological conditions [4–7]. As the poor tribological behavior is related to materials surfaces, surface engineering can be an effective approach to overcome such issues [7].

Among many surface engineering techniques, thermal oxidation (TO) has proven a cost-effective and efficient technique to engineer the surfaces of titanium and its alloys to improve their surface properties [5, 8, 9], including tribological properties [5, 9–12], corrosion resistance [11, 13, 14], tribocorrosion properties [15, 16], and biotribological properties [17, 18]. TO treatments are normally carried out at temperatures between 550 °C and 900 °C for various durations, ranging from less than 1 h to 100 h. Due to titanium's high affinity with oxygen and its ability to dissolve a large amount of oxygen in its crystal lattice, TO results in the formation of a TiO₂ oxide layer at the surface and an oxygen diffusion zone at the subsurface [19, 20]. The oxide layer, mostly with rutile structure, can offer anti-galling ability, low and stable friction and enhanced wear resistance [5, 11, 21], while the oxygen diffusion zone, which is hardened by solid solution hardening, can offer good wear resistance and load bearing capacity [22–24]. Ideally, a thick and adherent oxide layer on a thick oxygen diffusion zone should be achieved during TO in order to optimize the properties of TO treated titanium. However, there is always a limit in what can be achieved during TO treatments. At high TO temperatures, a thick oxide layer can be formed easily, but such an oxide layer is fragile and has poor adhesion with the oxygen diffusion zone and thus has limited practical tribological applications. Thus, for tribological applications, TO treatments of titanium and its alloys are mostly carried out at temperatures between 600 °C and 700 °C for several hours to several tens of hours, resulting in an adherent but relatively thin oxide layer at the surface and an oxygen diffusion zone up to 20 μm thick at the subsurface [5, 21].

The tribological properties of TO treated Ti and its alloys have been studied by many investigators under various environmental conditions, including dry [10, 12, 21, 25], oil lubrication [9, 11], corrosive solutions [15–18], and high temperatures [22, 26, 27]. Most of the

reported work were conducted between a TO treated titanium specimen and a counter-body made of other materials, such as a ceramic, a steel and a polymer counter-body. All the reported results demonstrate that TO is effective in improving the wear resistance of titanium and its alloys by as little as 25% up to as high as 4 orders of magnitude, depending on the wear test and TO treatment conditions [12, 21, 27]. Some of reported tests were conducted under relatively large loads, resulting in the wearing-through of the oxide layer and even the oxygen diffusion zone [12, 25, 28], where the measured wear properties were not characteristic of the oxide layer and the oxygen diffusion zone, but of the composite system. Under light loading conditions where the oxide layer and oxygen diffusion zone were not worn-through, it has been shown that the oxide layer has extremely good wear resistance, which could be more than 2 orders of magnitude better than untreated titanium [17, 21, 29]. There are also reports that TO treated titanium can reduce wear of the counter-body [30, 31]. For example, a TO treated titanium disc can reduce the wear of a UHMWPE pin by 2–3.5 times as compared to sliding against an untreated Ti disc [31]. Regarding the effect of TO on the coefficient of friction (COF) of titanium, inconsistent results have been reported by different investigators, probably due to the complex nature of friction and different counter-bodies and testing conditions employed. There are reports that TO can reduce COF [17, 18], does not influence COF and even increases COF of titanium sliding against other counter-bodies [10, 12, 32]. But when tested under light loading conditions, it has been clearly shown that the oxide layer can offer relatively low and stable friction, and when the oxide layer was worn-through, the TO treated specimen lost its friction-reducing ability [21].

Most of the reported tribological tests have been conducted between a TO treated specimen sliding against a counter-body made of other materials. There have been very few reports on the tribological behaviour of self-mating TO treated titanium, i.e., TO treated titanium sliding against TO treated titanium [33]. Tribologically, same material contacts should be avoided in order to minimize adhesion between the contacting bodies. However, in reality, many engineering applications involve same material combination, i.e., self-mating, such as in gears, bearings, valves and some biomedical applications, where galvanic corrosion maybe an issue. Durante et al. [33] studied the effect of TO treatment on different Ti6Al4V tribopairs, including the TO treated Ti6Al4V on TO treated Ti6Al4V pair. It was demonstrated that TO was effective in reducing friction and increasing wear resistance of the pair. Due to the limited test conditions and observations, the roles of the oxide layer and oxygen diffusion zone in friction and wear were not

clearly identified. In the present work, the effect of TO treatment on the dry sliding friction and wear behaviour of commercially pure titanium (CP-Ti) tribopairs has been investigated under a wide range of contact loading conditions ranging from elastic to plastic contacts. Three contact pairs have been investigated, including (1) the untreated Ti on untreated Ti pair, (2) the untreated Ti on TO treated Ti pair, and (3) the TO treated Ti on TO treated Ti pair. No such work has been reported for thermally oxidized CP-Ti. This work would provide a useful reference guide for the selection of contact pair for potential applications, such as for making light weight gears and bearings.

2 Materials and methods

2.1 Materials and thermal oxidation treatment

Commercially pure titanium (CP-Ti) grade 2 was used as the substrate material in this work. The material was received in the annealed state with the following chemical composition (in wt%): 0.08C, 0.24Fe, 0.03N, 0.21O, 0.014H, and balance Ti. Two geometrical forms were received: one in the form of a flat plate of 1.2 mm thickness, and another in the form of balls of 8 mm diameter with a surface finish of 0.05 μm (R_a). Disc specimens of 20 mm × 20 mm dimensions were cut from the flat plate. The flat surfaces of the specimens were then manually ground using SiC grinding papers down to the P1200 grade and polished in a silica colloid to achieve a mirror-like surface finish of 0.05 μm (R_a). No further surface polishing was applied to the as-received CP-Ti balls.

Thermal oxidation (TO) of the disc specimens and spherical ball specimens was carried out in the same batch in an air muffle furnace (Carbolite AAF 1100, UK) at 625 °C for 20 h. The heating rate was 20 °C min⁻¹. After TO, the specimens were allowed to cool in the furnace down to room temperature, which took around 8 h. Such a TO condition was determined previously to provide the optimal tribological performance when the oxidized disc was sliding against an alumina (Al₂O₃) ball slider [21], thus the same treatment condition was selected in this

work. After TO, the layer morphology of the oxidized specimen was characterized by microscopically examining metallographic sections, the phase composition was analyzed by X-ray diffraction (XRD) (Rigaku, Japan) using Cu-K_α radiation, and the surface hardness was measured under various indentation loads using a micro-hardness tester (Indentec ZHV, Germany). The results are presented in Sect. 3.1.

2.2 Dry sliding friction and wear tests

Dry and unlubricated sliding friction and wear tests were conducted using a laboratory scale reciprocating tribometer under ball-on-disc configuration, where the flat disc specimen was reciprocating linearly against a contacting stationary ball at controlled contact load, reciprocating frequency and stroke length. The friction force during sliding was measured by an incorporated load cell, which has been calibrated regularly according to manufacturer's instructions. In this work, all tests were conducted at a reciprocating frequency of 1 Hz and a stroke length of 7 mm for a duration of 3600 s, resulting a total sliding distance of 50.4 m. All tests were duplicated to ensure result consistency, i.e., two tests were conducted under each test condition.

Five contact loads were applied, including 0.25 N, 0.5 N, 1 N, 2 N and 4 N. These applied loads were smaller than those employed in most of the work reported in the literature. Employing small loads allowed for the determination of the response the thin oxide layer and the oxygen diffusion zone to dry sliding without excessive direct contribution from the substrate. Table 1 lists the initial maximum contact pressure, the maximum von Mises stress and its location and the contact radius under each load, calculated based on the Hertzian contact between a CP-Ti ball (8 mm diameter) and a CP-Ti flat (Young's modulus: 105 GPa, Poisson's ratio: 0.37). For the contacts between a TO treated ball and a TO treated disc and between an untreated Ti ball and TO treated disc, the contact analysis was performed by the finite element method. An axisymmetric FEA model was developed in

Table 1 Calculated Hertzian contact pressure (P_o), maximum von Mises stress (σ_{maxVM}), contact radius (a) and depth at which the maximum von Mises stress occurs (z) under the applied contact loads for the three contact pairs

Load (N)	P_o (MPa)			σ_{maxVM} (MPa)			a (μm)			z (μm)		
	Ti-Ti	Ti-TO	TO-TO	Ti-Ti	Ti-TO	TO-TO	Ti-Ti	Ti-TO	TO-TO	Ti-Ti	Ti-TO	TO-TO
0.25	219	220	221	130	131	132	24.1	23.9	23.9	11.9	10.9	11.0
0.5	276	277	278	164	165	166	30.2	29.9	29.9	14.9	13.9	13.9
1	348	349	350	206	207	208	38.0	37.8	37.8	18.9	17.9	17.9
2	438	439	441	260	261	262	48.0	46.8	46.8	22.9	22.9	22.9
4	552	553	554	328	328	329	60.2	59.7	59.7	29.9	28.9	28.9

ANSYS (R2022R1) to simulate the contact between a ball and a flat with a 1 μm thick oxide layer (Young's modulus: 230 GPa, Poisson's ratio: 0.27). The oxide layer was assumed to be perfectly adhered to the subsurface material. A Lagrangian contact method with no friction was used to prevent surface penetration. The ball was subjected to a vertical force ranging from 0.25 to 4 N, while the flat was constrained at the base (boundary condition). A variable mesh was employed to improve the computational efficiency, with a finer mesh in the regions of interest and a coarser mesh in the less important regions. The mesh sensitivity studies verified the adequacy of the model. The obtained results are also listed in Table 1. The results show that due to the small thickness of the oxide layer, the contact pressures and stresses were around 1% larger than those calculated for the untreated Ti ball on untreated Ti disc contact. In real applications, engineering components are rarely used under bulk plastic contact conditions. For the CP-Ti with a hardness of 180 HV and a yield strength of 315 MPa, according to the von Mises criterion, the contact loads of 0.25 N to 2 N resulted in bulk elastic contact between the ball and the flat, while the contact load of 4 N resulted in bulk plastic contact. Thus, the contact load range employed in this work allowed for the measurement of sliding friction and wear behaviour under both initial elastic and plastic contact conditions. It should be pointed out that the contact pressure and stress will change during the dynamic sliding wear process due to asperity contacts and changes in contact areas and surface conditions.

Three contact pairs were tested under the above testing conditions. These include.

- (1) untreated CP-Ti ball on untreated CP-Ti disc (Ti-Ti pair), i.e., self-mating untreated Ti;
- (2) thermally oxidized CP-Ti ball on thermally oxidized CP-Ti disc (TO-TO pair), i.e., self-mating TO treated Ti; and
- (3) untreated CP-Ti ball on thermally oxidized CP-Ti disc (Ti-TO pair), i.e., mating between untreated Ti and TO treated Ti.

2.3 Specimen characterization

After friction and wear tests, the wear scars on the balls and wear tracks on the discs were examined microscopically under an optical microscope (Nikon LV150N, Japan) and the sizes of the scar and the track were measured. The extended-depth-of-focus function of the Nikon microscope allowed for the capture of a series of focused images along the depth of the wear scar and wear track to construct 3D images and to measure surface profiles in local areas. A scanning electron microscope (SEM) (Carl Zeiss EVO LS 15, Germany) equipped with EDX facilities

was also used to examine selected wear scars and tracks. The wear depth from the ball was calculated from the measured mean diameter of the wear scar. The wear volume from the disc was estimated by measuring the surface profiles across the wear track in three locations using a profilometer (Surtronic Intra Touch, Taylor-Hobson, UK). This allowed for the calculation of the cross-sectional area of the wear track to obtain the wear volume. The wear rate (mm^3m^{-1}) was then obtained by dividing the wear volume (mm^3) by the total sliding distance (m).

3 Results and discussion

3.1 Structural characterization of TO specimen

From Fig. 1a it can be clearly seen that the TO treated CP-Ti comprised three distinct zones, i.e., an oxide layer (OL) about 1 μm thick at the surface which had a dark grey appearance, an oxygen diffusion zone (ODZ) of 8.5 μm thick below the oxide layer, and the substrate. Since oxygen is an α -phase stabilizing element which can cause interstitial solid solution hardening, the oxygen diffusion zone showed distinct features different from the underlying substrate. The XRD pattern shown in Fig. 1b confirmed that the oxide layer at the surface was rutile TiO_2 , and the α -phase peaks from the oxygen diffusion zone were all shifted towards lower diffraction angles, due to the dissolution of oxygen in the HCP lattice, leading to lattice expansion [34]. Such structural features of TO treated titanium have been reported by many investigators [16, 21, 35]. Due to the formation of the oxide layer and the oxygen diffusion zone, the surface hardness of CP-Ti was significantly increased, as shown in Fig. 1c. At the small indentation load of 0.025 kg, the surface hardness of the TO specimen was around 1100 $\text{HV}_{0.025}$, which was much higher than that of the untreated specimen (230 $\text{HV}_{0.025}$). This is in agreement with the results reported by other investigators [8, 12]. With increasing indentation load, the surface hardness of the TO specimen declined quickly up to 0.2 kg load and then declined slowly under further increasing load (Fig. 1c). This can be explained by the increasing contribution of the oxygen diffusion zone and then of the soft substrate.

3.2 Dry sliding friction and wear behaviour of the tribopairs

Figure 2 shows the coefficient of friction (COF) curves recorded under various contact loads for the three contact pairs and the calculated average COF for two duplicated tests under each load. The measured wear rates from the disc specimens are shown in Fig. 3. In the following sections, these results are interpreted and discussed for each contact pair in association with microscopic examinations of the wear scars on the balls and wear tracks on the discs.

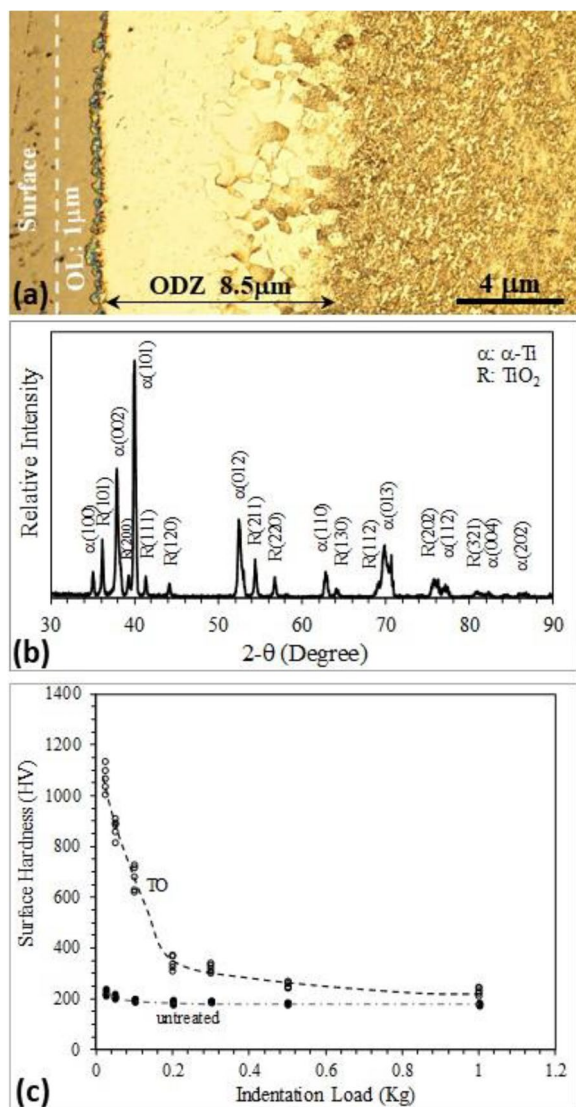


Fig. 1 Thermally oxidized (TO) Ti specimen: **a** metallographic section of the TO specimen showing the 1 μm thick oxide layer (OL) and the underneath 8.5 μm thick oxygen diffusion zone (ODZ), **b** X-ray diffraction pattern showing the rutile structure of the OL (Cu-K_α radiation), and **c** surface hardness as a function of indentation load

3.2.1 The untreated Ti ball-on-untreated Ti disc contact pair (Ti-Ti)

The untreated Ti ball-on-untreated Ti disc sliding contact (Ti-Ti) resulted in relatively high friction and large frictional fluctuations, where the COF values fluctuated largely throughout the sliding period (Fig. 2a). High friction was measured at the very beginning of each test without an obvious running-in stage. The COF curves measured at different loads showed similar behaviour, characterized by the large frictional fluctuations and the lack of a running-in stage. Although under the small

contact loads of 0.25 N to 2 N, initial elastic contact was expected (Table 1), the COF curves measured were similar to that measured at the largest load (4 N) where initial plastic deformation was expected. This suggests that similar wear mechanisms operated under all contact loads, irrespective of the initial contact deformation behaviour. As discussed below, adhesive and abrasive wear mechanisms dominated under all loading conditions.

From Fig. 2a, it can also be seen that there was a weak dependence of COF value on contact load. The average COF decreased slowly with increasing load (Fig. 2d), which could be related to the load dependence of the adhesion junctions formed at the contact interface [36]. Since frictional force is proportional to the normal load, as the load is increased, frictional force is also increased. This would result in increased frictional heating at the contact interface, which could reduce the shear strength of the adhesion junctions, and thus could result in smaller COF. Among the three contact pairs, the Ti-Ti pair showed the smallest COF values under contact loads ≥ 1 N (Fig. 2d). The measured COF values in this work for Ti-Ti contact is slightly smaller than those measured for Ti-ceramics and Ti-steel contacts [1].

Although the Ti-Ti pair showed the smallest COF values when the applied load was ≥ 1 N, such a contact pair experienced the largest amounts of wear from the disc specimen (Fig. 3) and the ball specimen (Fig. 4f). In Fig. 3a, the wear rate from the disc specimen was plotted against load. A linear relationship was found for the untreated Ti disc, suggesting again similar wear mechanisms under different loads. The wear rates from the untreated Ti discs were one to two orders of magnitude larger than those from the TO treated discs in the other two contact pairs (Fig. 3b).

Figure 4 shows the wear scars on the untreated Ti balls and the wear depth in the scar as a function of load. Figure 5 shows the wear tracks on the untreated Ti disc specimens and the measured surface profiles across the wear tracks. All the wear scars (Fig. 4) and wear tracks (Fig. 5) showed similar morphological features irrespective of applied load, confirming the earlier proposition that similar wear mechanisms operated under all loading conditions. The sizes of the scars and tracks increased with increasing load. The wear scars and tracks were characterized by the existence of scratch marks, material transfer and adhesion junction formation, as can be more clearly seen in Fig. 6. In addition to the scratch marks resulting from abrasive wear, there were prowls, craters, cracks, and fibrous torn areas on the worn surfaces, typical of adhesive wear (Fig. 6). As a result, the worn surfaces were very rough, as can be seen from Fig. 6 and the measured surface profiles shown in Fig. 5f, and large amounts of materials were removed from the untreated

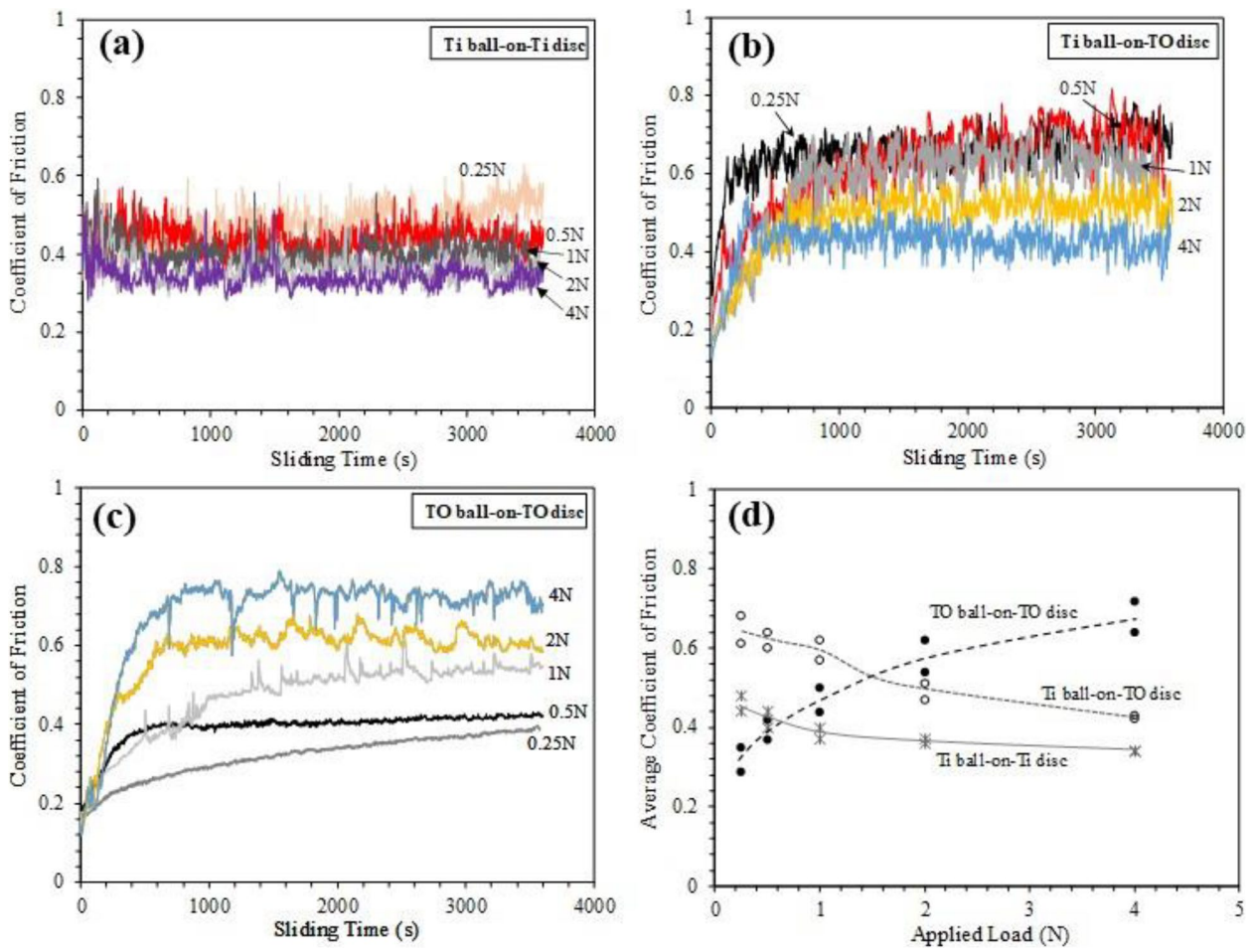


Fig. 2 Recorded coefficient of friction (COF) curves under various loads: **a** untreated Ti ball-on-untreated Ti disc, **b** untreated Ti ball-on-TO treated disc, **c** TO treated ball-on-TO treated disc, and **d** comparison of average COF of the three contact pairs

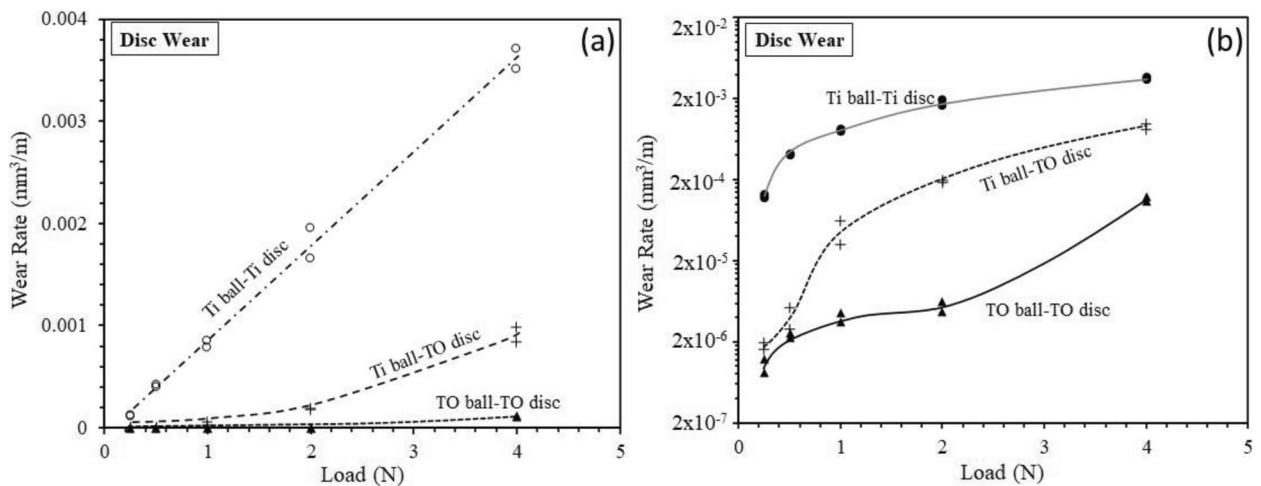


Fig. 3 Wear rate (WR) from the disc specimen as a function of load, resulting from the three contact pairs: **a** WR in linear scale, and **b** WR in logarithmic scale

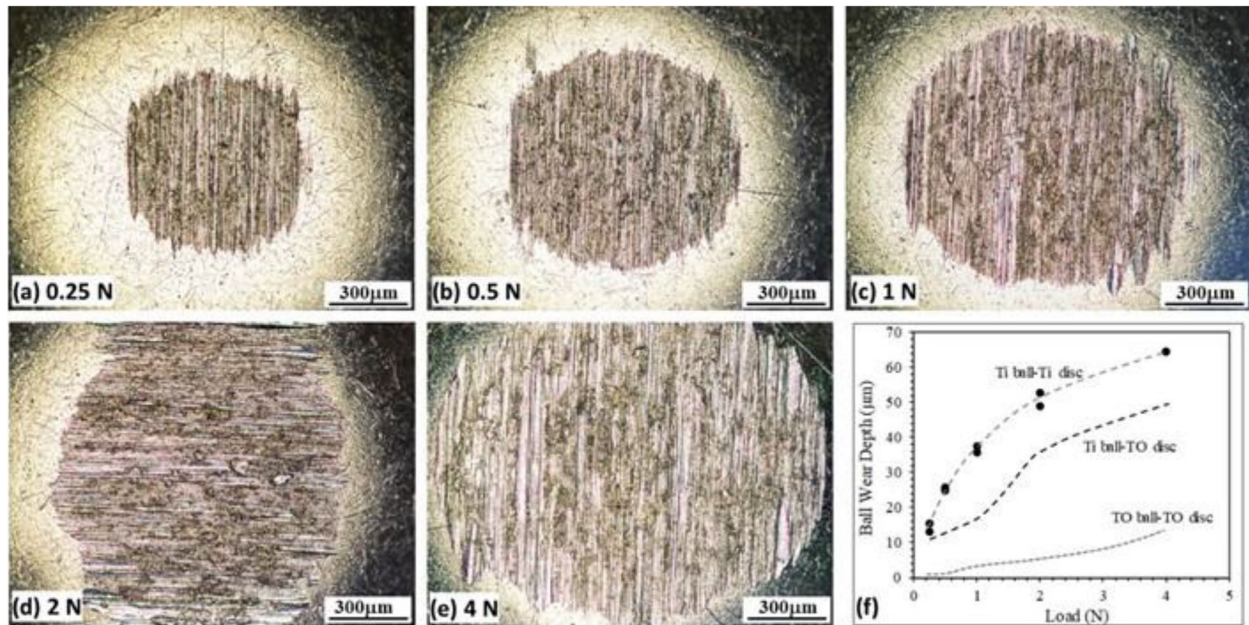


Fig. 4 Untreated Ti ball-on-untreated Ti disc: wear scars on the Ti ball after sliding against the Ti disc at various loads from 0.25 N to 4 N ((a) to (e)), and calculated ball wear depth as a function of load (f)

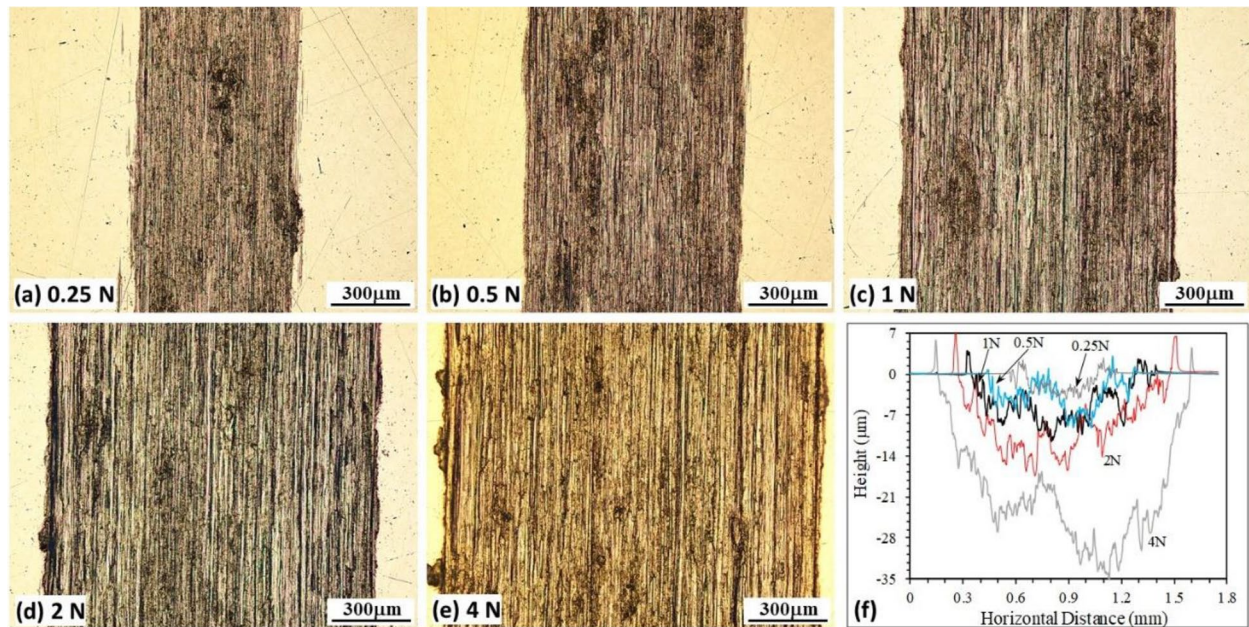


Fig. 5 Untreated Ti ball-on-untreated Ti disc: wear tracks on the Ti disc after sliding against the Ti ball at various loads from 0.25 N to 4 N ((a) to (e)), and surface profiles across the wear tracks produced at various loads (f)

Ti disc (Fig. 3) and the untreated Ti ball (Fig. 4f). The principal wear mechanisms are thus adhesive wear and abrasive wear, which lead to severe wear, typical of titanium and its alloys sliding against itself or other materials [1–3].

3.2.2 The untreated Ti ball-on-TO treated Ti disc contact pair (Ti-TO)

From the results presented in Sect. 3.2.1, it can be seen that the untreated Ti-on-untreated Ti contact represents a poor tribological pair which results in unstable

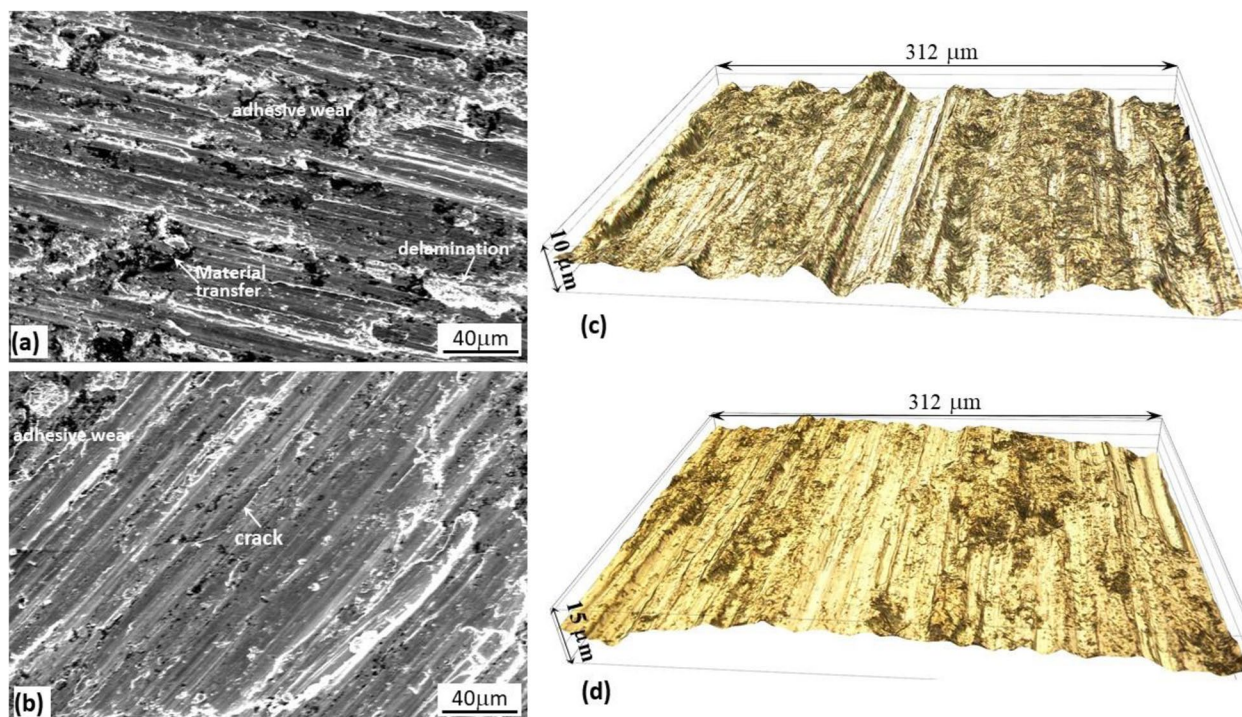


Fig. 6 Ti ball-on-Ti disc: SEM images showing **a** the wear scar on the Ti ball and **b** wear track on the Ti disc after sliding at 1 N load, and 3D images of the wear scar on the Ti ball **c** and wear track on the Ti disc **d** after sliding at 2 N load, showing adhesive and abrasive wear

friction and severe wear. Attempts were thus made to TO the disc specimen with the purpose to mitigate such a poor tribological behaviour, as discussed in this section.

From the COF curves shown in Fig. 2b, it can be seen that this contact pair experienced a running-in stage during the early stage of sliding where the COF started with low values and increased during the first 400 s of sliding to reach a steady-state. The COF curves were rather similar to those observed for the Ti–Ti pair with large COF fluctuations. The average COF was larger than those of the Ti–Ti pair, and declined with increasing load to approach the values of the Ti–Ti pair (Fig. 2d). In particular, under the small loads of 0.25 N to 1 N, the COF values of the Ti–TO pair was much larger than those of the Ti–Ti pair, which can be explained by the transfer of oxide from the TO treated disc to the untreated Ti ball (as discussed below). The wear rates from the TO treated disc (Fig. 3) and wear depths from the Ti ball (Fig. 7f) were smaller than those from the Ti–Ti pair. Under 0.25 N and 0.5 N loads, the wear rates from the TO treated disc were nearly two orders of magnitude smaller than those from the untreated Ti disc in the Ti–Ti pair (Fig. 3). Thus, thermally oxidizing the disc specimen helped to improve the wear resistance of both the disc and Ti ball specimens (Figs. 3 and 7f).

Figures 7 and 8 show the wear scars on the untreated Ti balls and wear tracks on the TO treated discs, respectively. The wear scars produced on the Ti balls under loads between 0.25 N and 1 N had similar features, including parallel deep abrasion marks and transfer of oxide materials from the TO treated disc to the untreated ball. Figure 9a is an enlarged view of the wear scar on the Ti ball produced under 0.5 N load. Clearly, oxide wear products were transferred from the disc to the ball to form a discontinuous compact film under the contact pressure, as further confirmed by SEM examination (Fig. 9b). EDS elemental mapping (Fig. 9c & d) confirmed that the compact film was rich in oxygen. EDS analysis of point A and point B in Fig. 9b showed that the oxygen content in point A was 31 wt% and that in point B was 12 wt%. Such material transfer was responsible for the high friction measured under loads between 0.25 N and 1 N (Fig. 2b & d). Under these contact loads, wear of the TO treated disc mainly occurred in the oxide layer as can be seen from Fig. 8a, b & c. Thus, the contact was Ti-on-oxide layer, which resulted in high friction. Under 0.25 N load, the oxide layer maintained its integrity and the wear track showed a polished appearance (Fig. 8a). Thus, the oxide layer was worn by micro-abrasion and polishing. When the load was increased to 0.5 N, the oxide layer mostly maintained its integrity, but suffered from flaking

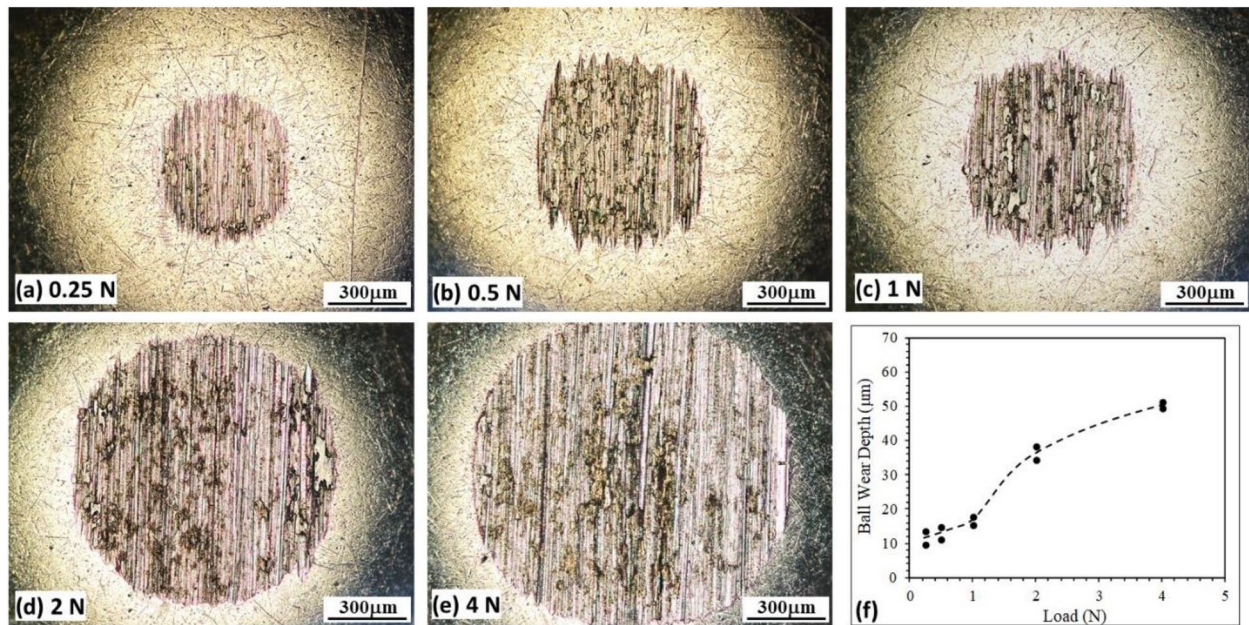


Fig. 7 Ti ball-on-TO disc: wear scars on the Ti ball after sliding against the TO disc at various loads from 0.25 N to 4 N ((a) to (e)), and calculated ball wear depth as a function of load (f)

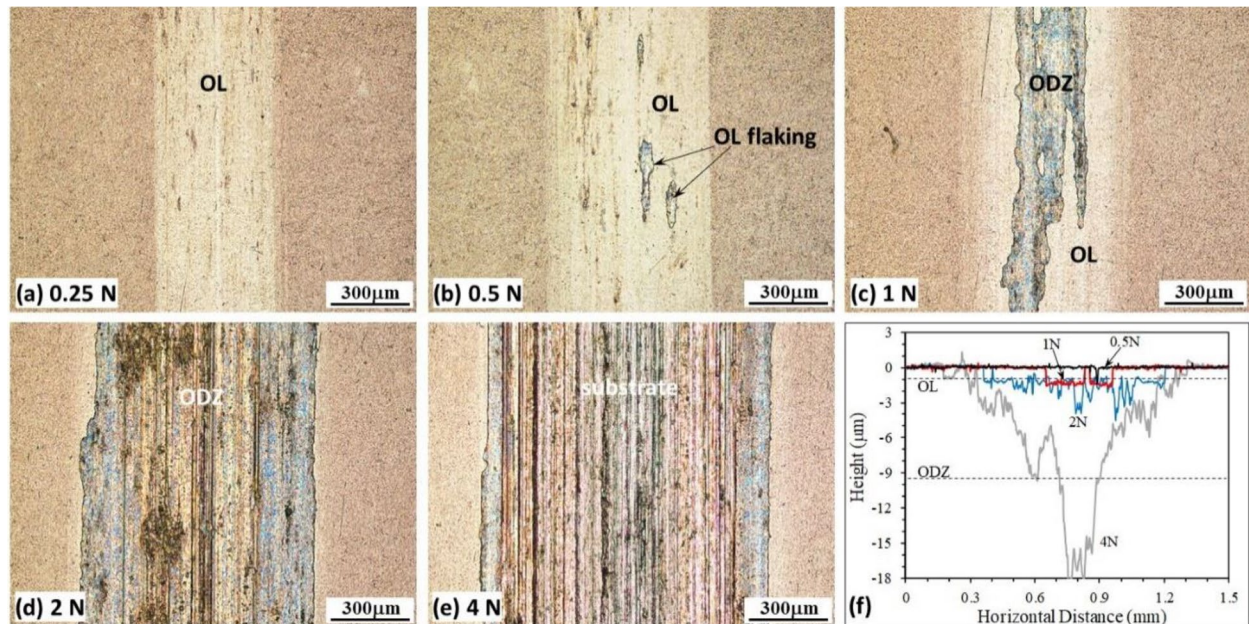


Fig. 8 Ti ball-on-TO disc: wear tracks on the TO disc after sliding against the Ti ball at various loads from 0.25 N to 4 N ((a) to (e)), and surface profiles across the wear tracks produced at various loads (f)

in some areas (Fig. 8b). The flaking areas increased when the load was further increased to 1 N, where the oxide layer in the central region of the wear track was removed (Fig. 8c). Under the larger load of 2 N (Fig. 8d), the oxide layer was completely removed, resulting in the contact

between Ti and the oxygen diffusion zone. Thus, material loss from the disc was mainly due to the flaking of the oxide layer. Under the further larger load of 4 N (Fig. 8e), the oxygen diffusion zone was removed (see Fig. 8f), resulting in Ti–Ti contact. Thus, the gradual decline of

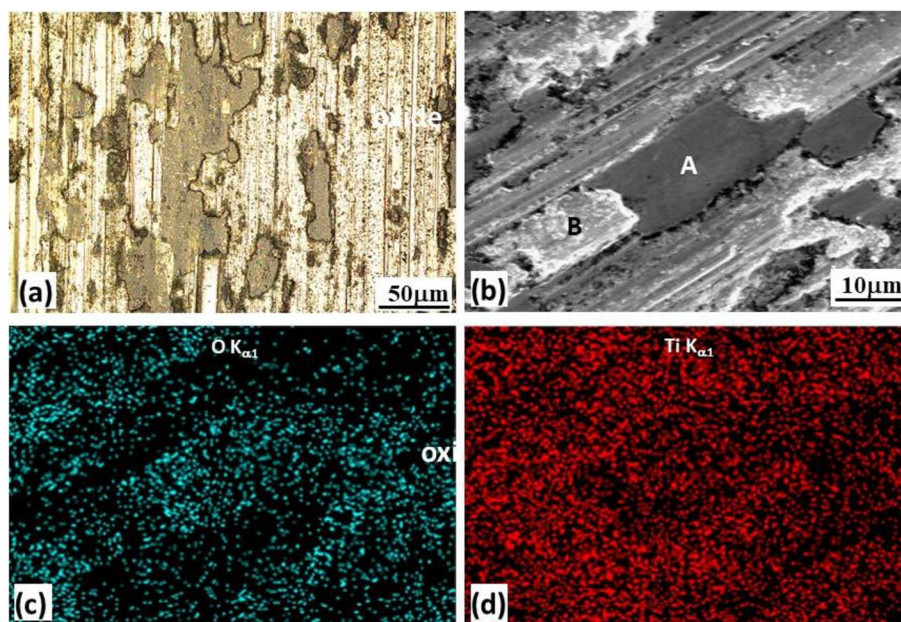


Fig. 9 Ti ball-on-TO disc: **a** enlarged view of the wear scar on the Ti ball produced under 0.5 N load showing the transfer of oxide from the TO disc to the ball, **b** SEM image showing the transferred oxide, **c** and **d** EDS oxygen and titanium elemental mappings of the area shown in **(b)**

COF with increasing load for the Ti-TO pair (Fig. 2d) can be explained as follows. At small contact loads, the oxide on the TO treated disc transferred to the untreated Ti ball, which was responsible for the high friction measured at 0.25 N to 1 N loads, as discussed above. With increasing load, the oxide layer was gradually removed from the disc, leading to reduced oxide transfer to the ball and thus reduced friction. When the oxide layer and oxygen diffusion zone were removed from the disc, the friction pair became similar to the Ti-Ti pair. Therefore, the COF of the Ti-TO pair gradually approached that of the Ti-Ti pair.

From the results presented in this section, it is clear that although the Ti-oxide layer contact resulted in high friction due to the transfer of oxide wear products to the Ti counter-face, it offered much improved wear resistance to both the untreated Ti ball and the TO treated Ti disc, as compared to the Ti-Ti pair. Only when the oxide layer was removed completely from the disc specimen was wear accelerated from both the disc and the ball. Further attempts were made to TO both the disc and ball specimens in order to further improve the tribological performance, as demonstrated in the following section.

3.2.3 The TO treated Ti ball-on-TO treated Ti disc contact pair (TO-TO)

The COF curves of the TO treated Ti ball-on-TO treated Ti disc pair (TO-TO) shown in Fig. 2c are completely different from those of the other two pairs shown in Fig. 2a

and b respectively. Firstly, there was a running-in stage in the TO-TO pair, where the COF started with a low value (below 0.2) and then increased with increasing sliding time to reach a steady-state (Fig. 2c). Secondly, there was a strong dependence of friction on load in the TO-TO pair, suggesting changes in wear mechanisms. Under the small loads of 0.25 N and 0.5 N, the COF curves were smooth with relatively low values. When the applied load was ≥ 1 N, the COF initially increased smoothly with sliding time, and then transitioned to a more erratic behaviour with spikes and valleys (Fig. 2c). As discussed below, such a behaviour was associated with the breakdown of the oxide layer on the ball and the trapping of the oxide particles at the contact interface. From Fig. 2d, it is clear that the average COF of the TO-TO pair increased with increasing load. Under the small loads of 0.25 N and 0.5 N, the average COF of the TO-TO pair was smallest among the three contact pairs, but under larger loads the TO-TO pair showed higher average COF than the Ti-Ti pair. This is due to the change in the contact interface after the oxide layer was broken down (see Sect. 3.3).

The most beneficial effect of the TO-TO pair is its good wear resistance, as shown in Figs. 3 and 4f. Under the small loads of 0.25 N and 0.5 N, where low friction was achieved, the wear rates from the TO treated disc were more than two orders of magnitude smaller than those from the untreated Ti disc in the Ti-Ti pair and 75% smaller than those from TO treated disc in the Ti-TO pair. Such a good wear resistance was

maintained under the larger contact loads of 1 N and 2 N, although the contact pair experienced higher friction under these loads. Under the largest load of 4 N, the wear volume from the TO treated disc was increased significantly, but it was still more than one order of magnitude smaller than that from the Ti disc in the Ti–Ti pair and nearly one order of magnitude smaller than that from the TO disc in the Ti–TO pair (Fig. 3).

Figure 10 shows the wear scars on the TO treated balls and the wear depths of the scars calculated from the scar diameter. Figure 11 shows the wear tracks on the TO treated discs and the surface profiles measured across the wear tracks by profilometer. Under 0.25 N and 0.5 N loads, the wear scars on the TO treated balls (Fig. 10a & b) were small with wear depths below 1 μm (Fig. 10f), and the wear tracks on the TO discs (Fig. 11a & b) had shiny and polished appearances with hardly measurable wear. Thus, the contact under these two loads was oxide layer-on-oxide layer throughout the test, corresponding to the low and smooth friction (Fig. 2c) and very small amount of wear from both the ball and disc specimens (Figs. 3 and 10f). The principal wear mechanism was micro-abrasion and polishing between the oxide layers. The oxide layers, supported by the oxygen diffusion zones, effectively prevented adhesion between the ball and the disc. The COF values of around 0.35 for the TiO_2 - TiO_2 contact is similar to those reported for TiO_2 - Al_2O_3 contact [20] and larger than those reported in [33].

Under 1 N and 2 N loads (Fig. 10c & d), the wear scars on the TO balls showed two distinct regions: a central circular region with a shiny and polished appearance and an outer ring revealing the oxide layer. The wear depths in the wear scars were larger than 1 μm , but smaller than the thickness of the oxygen diffusion zone (Fig. 10f). The corresponding wear tracks on the discs still showed shiny and polished appearances without any sign of wearing-through of the oxide layer (Fig. 11c & d). Clearly, under these two loads, the oxide layer was worn through from the ball but not from the disc. Thus, the contact was oxide-on-oxide at the early stage of sliding, corresponding to the low, smooth and gradually increasing COF region in the friction curves (Fig. 2c). At the later stage of sliding, the contact was a mixture of oxygen diffusion zone-on-oxide layer (central region) and oxide layer-on-oxide layer (outer ring) after the oxide layer was worn-through on the TO treated ball, corresponding to the high and erratic friction region in Fig. 2c. It is believed that the erratic frictional behaviour was due to the local flaking of the oxide layer from the outer ring of the contact zone. Figure 12 is an enlarge view of the wear scar shown in Fig. 10c, showing a crater at the outer ring of the contact zone and the surface profile measured across the crater. The depth of the crater was similar to the thickness of the oxide layer. Obviously, the crater was formed due to flaking of the oxide layer. The trapping of the flaked oxide particles in the contact interface could cause sudden jumps

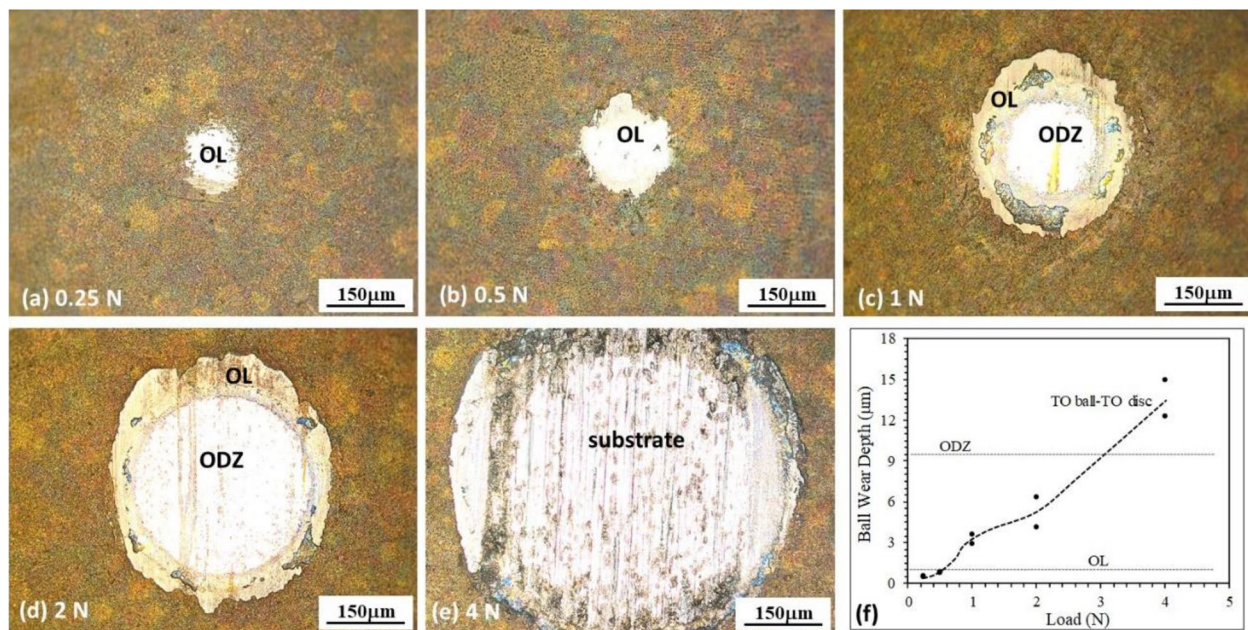


Fig. 10 TO ball-on-TO disc: wear scars on the TO treated ball after sliding against the TO treated disc at various loads from 0.25 N to 4 N ((a) to (e)), and calculated ball wear depth as a function of load (f)

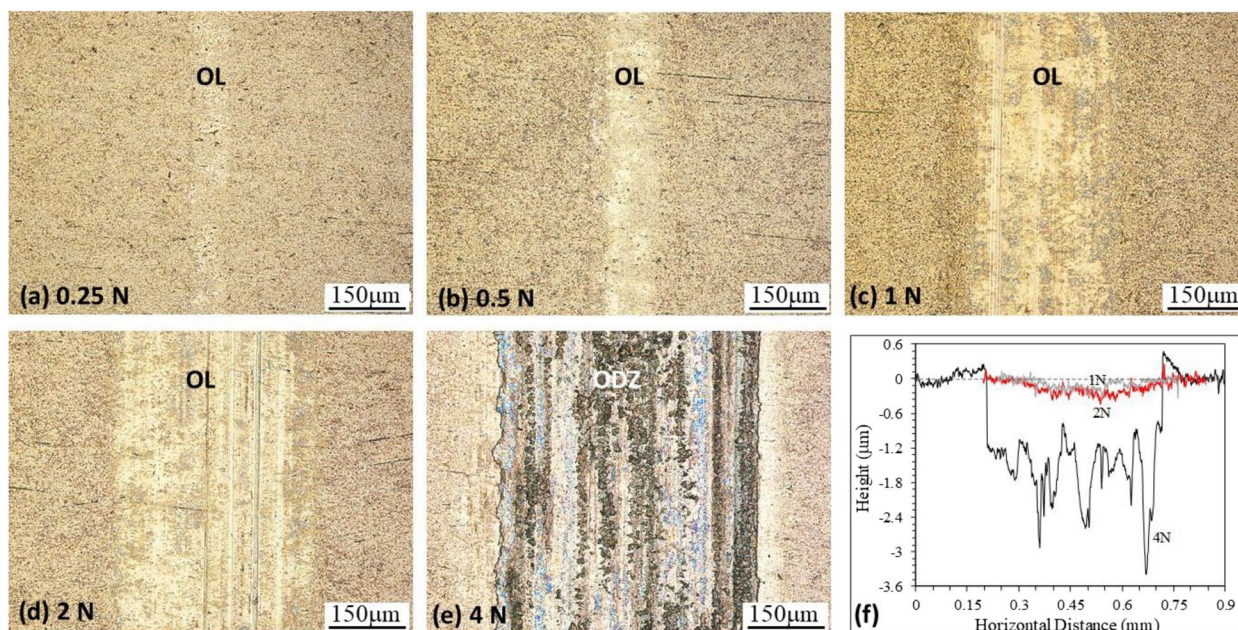


Fig. 11 TO ball-on-TO disc: wear tracks on the TO treated disc after sliding against the TO treated ball at various loads from 0.25 N to 4 N ((a) to (e)), and surface profiles across the wear tracks produced at various loads (f)

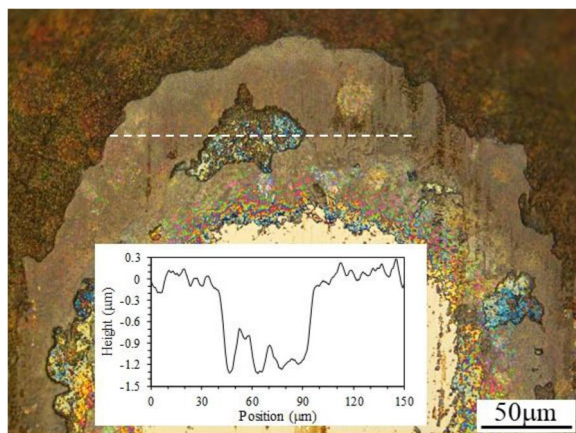


Fig. 12 TO ball-on-TO disc: enlarged view of the wear scar on the TO ball after sliding against the TO disc at 1 N load. The inset shows the surface profile measured across the area indicated by the dashed line, showing local removal of the oxide layer at the outer ring of the wear scar

in COF. It is interesting to note that the sliding between the oxide layer on the disc and the oxygen diffusion zone on the ball did not lead to accelerated wear of the disc since the oxide layer on the disc maintained its integrity with the substrate under these contact loads. The principal wear mechanisms were micro-abrasion and polishing of the disc and ball specimens, and oxide layer flaking from the ball specimen.

Under 4 N load, both the oxide layer and oxygen diffusion zone were worn through on the TO treated ball, resulting in a rough wear scar surface (Fig. 10e) and accelerated wear depth on the ball (Fig. 10f). On the corresponding disc specimen, the oxide layer was worn through in the wear track and wear occurred within the diffusion zone (Fig. 11e & f). As compared to the untreated Ti disc in the Ti-Ti pair, the wear volume from the TO treated disc in the TO-TO pair was more than one order of magnitude smaller (Fig. 3b). Thus, the oxygen diffusion zone can also offer good wear resistance, although it was not as good as the oxide layer.

From the results presented in this section, it is clear that the oxide layer-on-oxide layer contact (under 0.25N and 0.5 N) represents an ideal material combination to achieve excellent tribological properties under dry sliding conditions, in terms of reduced friction and much enhanced wear resistance. When compared with the Ti-TO pair where the oxide layer on the TO treated disc only survived up to 0.5 N load (Fig. 8), the oxide layer on the TO treated disc in the TO-TO pair survived up to 2 N load (Fig. 11). Thus, tribologically, the TO-TO pair performed much better than the Ti-TO pair. The untreated Ti ball caused more damage to the oxide layer on the TO treated disc than the TO treated ball did. It is thus essential to thermally oxidize both specimens in order to achieve optimal tribological performance.

3.3 Oxide layer failure mechanism

The above results and discussion demonstrate that once the oxide layer maintains its integrity with the oxygen diffusion zone on both the disc and ball specimens, the contact pair can offer low and stable friction and excellent wear resistance. Removal of the oxide layer from one of the bodies of the contact pair results in increased and unstable friction although the oxygen diffusion zone can still offer a certain degree of wear protection. Due to the importance of the oxide layer in maintaining good tribological properties, further analysis was carried out to study the failure mechanism of the oxide layer under TO-TO contact conditions.

Under 0.5 N load, the oxide layer on the ball (Fig. 10b) and the disc (Fig. 11b) was not worn through after sliding

for 3600 s. However, when examined under higher magnifications, it was found that some bulges were formed in some local areas of the wear scar on the ball (Fig. 13). These bulges have heights up to 1.5 μm . Obviously, in the bulging areas, the oxide layer was lifted from the underlying oxygen diffusion zone, suggesting the formation of interfacial cracks. Cracks were observed on the surface of some bulges, indicating the onset of local oxide layer flaking. It is thus expected that with increasing sliding time under 0.5 N load, the oxide layer would flake from the oxygen diffusion zone, leading to a change in frictional and wear characteristics similar to that observed under 1 N load.

The COF curve recorded for the TO-TO pair under 1 N load (Fig. 2c) shows two distinct regions, as illustrated

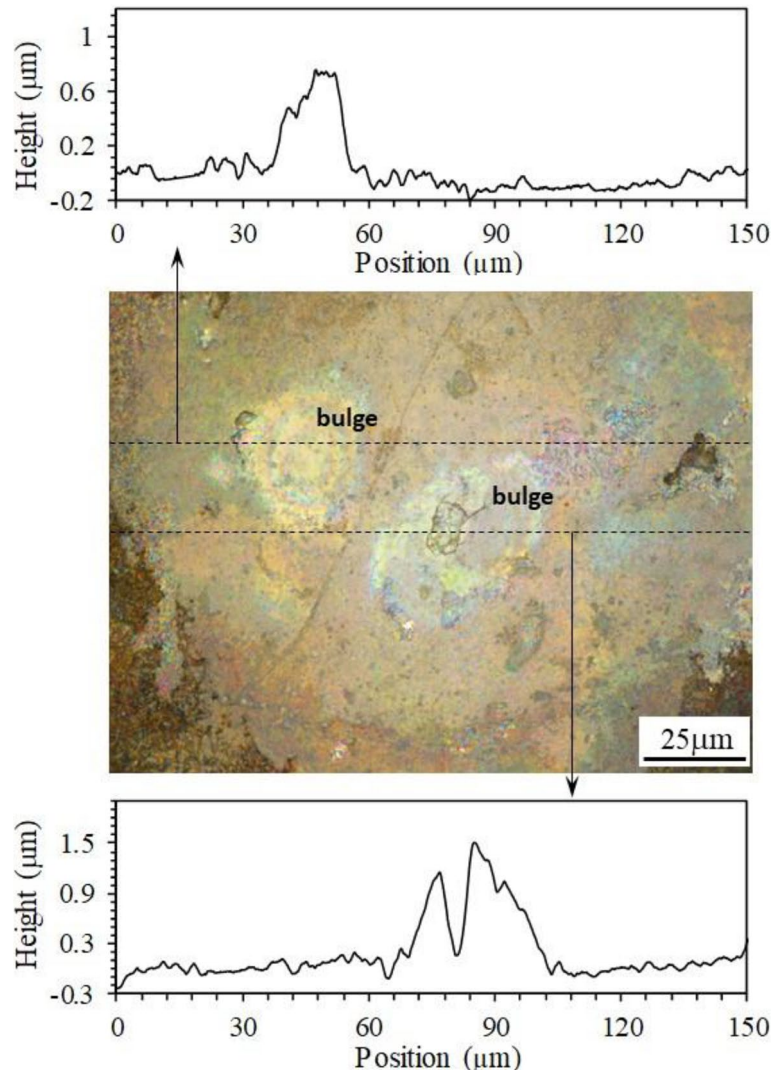


Fig. 13 TO ball-on-TO disc: enlarged view of the wear scar on the TO ball after sliding against the TO disc at 0.5 N load (Fig. 10b), and surface profiles measured across indicated areas, showing local bulging and cracking of the oxide layer in the contact zone

in Fig. 14a. In the first region during early stage of sliding for the first 500 s, the COF curve is smooth with an increasing trend. In the second region, the COF curve is more erratic with spikes. In order to understand the transition in frictional behaviour, further sliding tests for different times were done. After testing for 200 s, 480 s and 540 s respectively, the tests were stopped and the wear scars on the balls were examined, see Fig. 14. After testing for 200 s (Fig. 14b), which was in the smooth COF region, some bulges were already formed on the wear scar surface, suggesting interfacial crack formation at the early stage of sliding under 1 N load. After sliding for 480 s (Fig. 14c), which was just before the appearance of the first spike in the COF curve, the bulges increased in size and height with many cracks, signifying the onset of oxide layer failure. After sliding for 540 s (Fig. 14d), which was just after the appearance of the first spike, the oxide layer came off from the bulging area. It is thus clear that the COF spikes were caused by the flaking of the oxide layer in local areas due to the formation of interfacial cracks. With continuous sliding, more oxide layer would come off from the contact zone (see Fig. 12), leading to the formation of COF spikes at irregular intervals (Fig. 2c). Thus, the increase in COF with increasing load

for the TO-TO pair, shown in Fig. 2c & d, was due to the gradual flaking of the oxide layer from the TO treated ball specimen. The trapping of the flaked oxide particles at the contact interface led to increased friction and COF spikes.

Clearly, flaking of the oxide layer was initiated by the formation of interfacial cracks. Flaking of thin films is a common phenomenon that has been observed in many hard coating-soft substrate systems [37–41]. When the stress induced at the coating-substrate interface exceeds the adhesion strength of the coating, interfacial cracks would form and propagate, leading to coating flaking. Thus, the interfacial adhesion strength between the oxide layer and the oxygen diffusion zone would play an important role in maintaining the integrity of the oxide layer. The obvious approach to prolong the durability of the oxide layer and to increase its load bearing capacity is to improve the oxide layer-oxygen diffusion zone adhesion strength through process optimization. The TO condition employed in this work was based on previous work, optimized for the Al_2O_3 ball-on-TO treated Ti disc contact pair [21]. Further investigation is currently being carried out to further optimize the TO conditions for the excellent TO-TO tribo-pair.

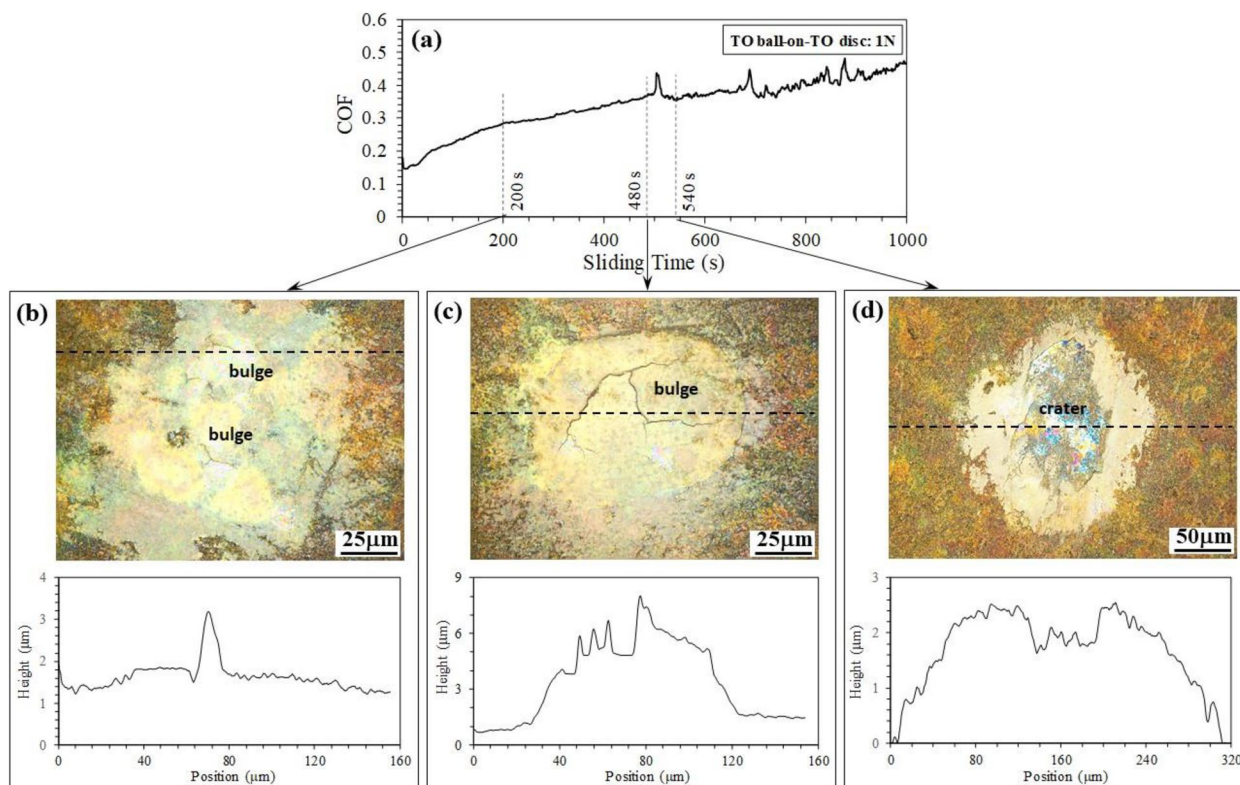


Fig. 14 TO ball-on-TO disc: zoom-in view of the friction curve recorded at 1 N load for the first 1000 s (a), and microscopic images of the wear scar on the TO ball and surface profiles across indicated areas, after sliding at 1 N for b 200 s, c 480 s and d 540 s, showing the gradual development of interfacial cracks which lead to the local bulging and flaking of the oxide layer in the contact zone on the TO ball

4 Conclusions

In this work, the dry sliding friction and wear behaviour of self-mating TO treated CP-Ti has been studied for the first time under a wide range of loading conditions, as compared to the Ti–Ti and Ti–TO contact pairs. The following conclusions can be drawn:

- (1) Among the three contact pairs studied, the TO–TO pair performs the best under dry sliding conditions, in terms of low friction and superior wear resistance. This is followed by the Ti–TO pair, with the Ti–Ti pair being the worst-performing tribo-pair. It is thus essential to thermally oxidize both specimens in order to achieve optimal tribological performance.
- (2) The oxide layer–oxide layer contact in the TO–TO pair under small contact loads results in low and stable friction with COF values below 0.4 and superior wear resistance of both the TO ball and TO disc. The wear resistance of the TO disc is more than two orders of magnitude higher than that of the Ti disc in the Ti–Ti pair, and is 70% better than the TO disc in the Ti–TO pair.
- (3) It is important to maintain the integrity of the oxide layer with the oxygen diffusion zone in the TO–TO pair during the sliding process. Once the oxide layer is removed from the TO treated ball under large contact loads or after prolonged sliding, the oxygen diffusion zone–oxide layer contact results in high and unstable friction, but still offers good wear resistance to the TO treated disc.
- (4) The contact between an untreated Ti ball and a TO treated disc is not as good as the contact between a TO treated ball and a TO treated disc. The Ti–oxide layer contact results in high friction with large fluctuating COF values, due to the transfer of the oxide from the disc to the ball.
- (5) The oxide layer on the TO treated disc in the TO–TO pair has better load bearing capacity than the oxide layer on the TO treated disc in the Ti–TO pair. The former can survive up to 2 N contact load, while latter can only survive up to 0.5 N contact load. The untreated Ti ball causes more damage to the TO disc than the TO treated ball does.
- (6) Failure of the oxide layer in the TO–TO pair is initiated by the formation of interfacial cracks at the oxide layer–oxygen diffusion zone interface, which leads to the bulging and then flaking of the oxide layer. It is important to optimize the interfacial adhesion strength in order to enhance the integrity of the oxide layer during the dry sliding wear process.

Acknowledgements

Authors acknowledge the Royal Society for providing the International Exchange programme.

Authors' contributions

Methodology, Y.S., J.Z., Y.L., X.J.; Experimentation, R.B., Y.S., Y.L.; Investigation, Y.S., J.Z., X.J., R.B.; Y.L. Writing – original draft preparation, R.B., Y.S.; Writing – review and editing, Y.S., J.Z., X.J.

Funding

This work was partially funded by the Royal Society International Exchange Programme, Ref. IES\R3\213006.

Availability of data and materials

The original data of this work is available from the authors upon reasonable request.

Declarations

Competing interests

Yong Sun is a member of the editorial board of this journal. He was not involved in the editorial review or the decision to publish this article. All authors declare that there are no competing interests.

Received: 8 September 2023 Revised: 16 October 2023 Accepted: 30 October 2023

Published online: 22 November 2023

References

1. Qu J, Blau PJ, Watkins TR, Cavin OB, Kulkarni NS (2005) Friction and wear of titanium alloys sliding against metal, polymer, and ceramic counterfaces. *Wear* 258:1348–1356
2. Budinski KG (1991) Tribological properties of titanium alloys. *Wear* 151:203–217
3. Molinari A, Straffelini G, Tesi B, Bacci T (1997) Dry sliding wear mechanisms of the Ti6Al4V alloy. *Wear* 208:105–112
4. Tian H, Saka N, Suh NP (1989) Boundary lubrication studies on undulated titanium surfaces. *Tribol Trans* 32:289–296
5. Dong H, Bell T (2000) Enhanced wear resistance of titanium surfaces by a new oxidation treatment. *Wear* 238:131–137
6. Yang Y, Zhang C, Dai Y, Luo J (2017) Tribological properties of titanium alloys under SEE oil and aqueous solutions. *Tribol Int* 109:40–47
7. Dong H (2010) Surface engineering of light alloys aluminium, magnesium and titanium alloys. Woodhead Publishing Limited, UK, p 662
8. Lin N, Xie R, Zou J et al (2019) Surface damage mitigation of titanium and its alloys via thermal oxidation: a brief review. *Rev Adv Mater Sci* 58:132–146
9. Yan W, Wang XX (2004) Surface hardening of titanium by thermal oxidation. *J Mater Sci* 39:5583–5585
10. Aniolek K, Kupka M, Barylski A (2016) Sliding wear resistance of oxide layers formed on titanium surface during thermal oxidation. *Wear* 356–357:23–29
11. Bloyce A, Qi PY, Dong H, Bell T (1998) Surface modification of titanium alloys for combined improvements in corrosion and wear resistance. *Surf Coat Tech* 107:125–132
12. Aniolek K, Barylski A, Kowalewski P, Kaptacz S (2022) Investigation of dry-sliding friction and wear and mechanical behavior of the Ti-6Al-7Nb alloy after thermal oxidation. *Materials* 15:3169
13. Kumar S, Sankara Narayanan TSN, Ganesh Sundara Raman S, Seshadri SK (2009) Thermal oxidation of CP-Ti: evaluation of characteristics and corrosion resistance as a function of treatment time. *Mater Sci Eng C* 29:1942–1949
14. Ahmed FS, El-Zomor MA, Abo Ghazala MS, Elshaer RN (2022) Effect of oxide layer formed by thermal oxidation on mechanical properties and NaCl-induced hot corrosion behaviour of TC21 Ti-alloy. *Sci Rep* 12:19265

15. Guleryuz H, Cimenoglu H (2004) Effect of thermal oxidation on corrosion and corrosion-wear behaviour of Ti-6Al-4V alloy. *Biomaterials* 25:3325–3333
16. Bailey R (2018) Tribocorrosion response of surface-modified Ti in a 0.9% NaCl solution. *Lubricants* 6:86
17. Wang S, Liu Y, Zhang C, Liao Z, Liu W (2014) The improvement of wettability, biotribological behavior and corrosion resistance of titanium alloy pretreated by thermal oxidation. *Tribol Int* 79:174–182
18. Luo Y, Chen W, Tian M, Teng S (2015) Thermal oxidation of Ti6Al4V alloy and its biotribological properties under serum lubrication. *Tribol Int* 89:67–71
19. Kumar S, Sankara Narayanan TSN, Ganesh Sundara Raman S, Seshadri SK (2010) Thermal oxidation of CP Ti – an electrochemical and structural characterization. *Mater Charact* 61:589–597
20. Aniolek K (2017) The influence of thermal oxidation parameters on the growth of oxide layers on titanium. *Vacuum* 144:94–100
21. Bailey R, Sun Y (2013) Unlubricated sliding friction and wear characteristics of thermally oxidized commercially pure titanium. *Wear* 308:61–70
22. Zhou Y, Zhang QY, Liu JQ, Cui XH, Mo JG, Wang SQ (2015) Wear characteristics of a thermally oxidized and vacuum diffusion heat treated coating on Ti-6Al-4V alloy. *Wear* 344–345:9–21
23. Dong H, Li XY (2000) Oxygen boost diffusion for the deep-case hardening of titanium alloys. *Mater Sci Eng A* 280:303–310
24. Borgioli F, Galvanetto E, Iozzelli F, Pradelli G (2005) Improvement of wear resistance of Ti-6Al-4V alloy by means of thermal oxidation. *Mater Let* 59:2159–2162
25. Aniolek K, Kupka M, Barylski A, Dercz G (2015) Mechanical and tribological properties of oxide layers obtained on titanium in the thermal oxidation process. *Appl Surf Sci* 357:1419–1426
26. Singh K, Ganesh Sundara Raman S (2023) High temperature sliding wear behaviour of Ti6Al4V thermal oxidised for different oxidation durations. *Met Mater Int* 29:357–368
27. Lou M, Alpas AT (2019) High temperature wear mechanisms in thermally oxidized titanium alloys for engine valve applications. *Wear* 426–427:443–453
28. Biswas A, Majumdar JD (2009) Surface characterization and mechanical property evaluation of thermally oxidized Ti-6Al-4V. *Mater Charact* 60:513–518
29. Guleryuz H, Cimenoglu, (2005) Surface modification of Ti-6Al-4V alloy by thermal oxidation. *Surf Coat Tech* 191(2005):164–170
30. Dong H, Shi W, Bell T (1999) Potential of improving tribological performance of UHMWPE by engineering the Ti6Al4V counterfaces. *Wear* 225–229:146–153
31. Prayoga BT, Suyitno S, Dharmastiti R (2016) The wear behavior of UHMWPE against surface modified CP-titanium by thermal oxidation. *Tribol Industry* 38(4):543–551
32. Maytorena-Sanchez A, Hernandez-Torres J, Lopez-Huerta F et al (2021) Analysis of hardness and tribological properties of grade 2 titanium using thermal oxidation process at different temperatures. *Mat Let* 282:128679
33. Durante M, Boccarusso L, Velotti C, Astarita A, Squillace A, Carrino L (2017) Characterization of Ti-6Al-4V tribopairs: effect of thermal oxidation. *J Mater Eng Perform* 26:571–583
34. Ashrafizadeh A, Ashrafizadeh F (2009) Structural features and corrosion analysis of thermally oxidized titanium. *J Alloys Compounds* 480:849–852
35. James M, Sankara Narayanan TSN, Chu PK (2013) Thermal oxidation of titanium: evaluation of corrosion resistance as a function of cooling rate. *Mater Chem Phys* 138:565–572
36. Ainbinder SB, Francs AS (1966) On the mechanism of the formation and destruction of adhesion junctions between bodies in friction contact. *Wear* 9:209–227
37. Arai T, Fujita H, Watanabe M (1987) Evaluation of adhesion strength of thin hard coatings. *Thin Solid Films* 154:387–401
38. Jiang J, Arnell RD (2000) The effect of substrate surface roughness on the wear of DLC coatings. *Wear* 239:1–9
39. Li H, Ma D, Wang H, Yun D, Hao Z, Deng J, Zhang R, Li Z (2023) Microstructure and oxidation behaviour of CrCN/TiSiCN nano-multilayer coatings on Zircalloy in high-temperature steam. *Corros Sci* 211:110883
40. Hintermann HE (1984) Adhesion, friction and wear of thin hard coatings. *Wear* 100:381–397
41. Liu J, Zhu SS, Liu JY, Wang ZP (2020) Cutting performance and wear behavior of AlTiN and TiAlSiN coated carbide tools during dry milling of Ti-6Al-4V. *Acta Metallurgica Sinica* 33:459–470

Publisher's Note

Springer Nature remains neutral with regard to jurisdictional claims in published maps and institutional affiliations.